FZJ-IKP-TH-2008-19, HISKP-TH-08-25

Quark mass dependence of the pion vector form factor

Feng-Kun Guo[1], Christoph Hanhart[1,2], Felipe J. Llanes-Estrada[3], Ulf-G. Meißner[1,2,4]

[1] *Institut für Kernphysik and Jülich Center for Hadron Physics, Forschungszentrum Jülich, D–52425 Jülich, Germany*
[2] *Institut for Advanced Simulations, Forschungszentrum Jülich, D–52425 Jülich, Germany*
3 *Departamento de Física Teórica I, Universidad Complutense de Madrid, 28040 Madrid, Spain*
[4] *Helmholtz-Institut für Strahlen- und Kernphysik (Theorie) and Bethe Center for Theoretical Physics, Universität Bonn, D–53115 Bonn, Germany*

Abstract

We examine the quark mass dependence of the pion vector form factor, particularly the curvature (mean quartic radius). We focus our study on the consequences of assuming that the coupling constant of the ρ to pions, $g_{\rho\pi\pi}$, is largely independent of the quark mass while the quark mass dependence of the ρ–mass is given by recent lattice data. By employing the Omnès representation we can provide a very clean estimate for a certain combination of the curvature and the square radius, whose quark mass dependence could be determined from lattice computations. This study provides an independent access to the quark mass dependence of the $\rho\pi\pi$ coupling and in this way a non-trivial check of the systematics of chiral extrapolations. We also provide an improved value for the curvature for physical values for the quark masses, namely $\langle r^4\rangle = 0.73 \pm 0.09$ fm^4 or equivalently $c_V = 4.00 \pm 0.50$ GeV^{-4}.

Key words: Pion form factor, Omnès representation, Quark mass dependence, Inverse Amplitude Method
PACS: , 11.10.St, 11.55.Bq, 12.39.Fe, 12.40.Vv, 13.40.Gp

1. Introduction and notation

The expectation value of the vector current between two pion fields may be written as

$$\langle \pi^\pm(p')|j^\mu|\pi^\pm(p)\rangle = (p+p')^\mu F_\pi^V(q^2) \ .$$

Since the only form factor that we discuss is the charged pion form factor, we will denote it simply as $F(q^2)$, where $q = p - p'$. It is conventionally normalized as $F(0) = 1$.

An expansion around zero momentum transfer allows for a physical interpretation of the form factor in terms of the pion's rest frame charge density $\rho(r)$, given by

$$F(t) = 1 + \frac{1}{3!}\langle r^2\rangle_\rho t + \frac{1}{5!}\langle r^4\rangle_\rho t^2 + \mathcal{O}(t^3) \ . \tag{1}$$

Here we used the notation of Ref. [1]. Alternatively, in Ref. [2] the curvature of the form factor was introduced via

$$F(t) = 1 + \frac{1}{6}\langle r^2\rangle t + c_V^\pi t^2 + \mathcal{O}(t^3) \ . \tag{2}$$

Comparing with Eq. (1) we see that

$$c_V^\pi = \frac{1}{5!}\langle r^4\rangle \ .$$

The first term in the form–factor expansion is the conventional charge normalization $\int d^3r\rho(r) = \langle 1\rangle_\rho = 1$, and the derivative at the origin provides the (vector or charge) pion radius $\langle r^2\rangle = 6(dF/dq^2)(0)$. At the next

Table 1
Current theoretical estimates of the pion's quartic radius . The lattice results are our estimate based on the form factor data from [15].

$\langle r^4\rangle/\langle r^2\rangle^2$	Method
3.3	VMD [2]
2 ± 2.5	Lattice $m_\pi = 0.33$ GeV [15]
2 ± 2.3	Lattice extrapolated to $m_\pi = 0.139$ GeV [15]
4 ± 2	NNLO χPT [16]
3.1 ± 0.4	Padé approximants [17]
3.6 ± 0.6	Eq. (7) this work

order, the non-relativistic interpretation should be modified as effects of boosting the pion wave function should begin to appear. In this article we will ignore this subtlety, and simply use equivalently the term pion's mean quartic radius or form factor curvature. We will mainly focus on this quantity. Using both chiral perturbation theory and dispersion relations we find a reliable value for the curvature.

Assuming that the $\rho\pi\pi$ coupling is largely independent of the quark masses for a given quark mass dependence of m_ρ, we can also predict the quark mass dependence of the curvature. The quark mass dependence of the ρ properties was studied in various recent lattice simulations [3,4] as well as using unitarized chiral perturbation theory [5].

Abundant data on the pion form factor exists, that can be obtained from the Durham reaction database. For the timelike form factor we use contemporary sets from the CMD2, KLOE, and SND experiments [6,7,8]. In addition there is higher energy data from Babar[9] that shows the $\rho(1700)$ and a shoulder that could correspond to the $\rho(1400)$. However, in our study we employ only the $\rho(770)$. We will therefore not extend our study beyond 1.2 GeV, where in addition $K\bar{K}$ and other inelastic channels start to contribute significantly. It is this condition that prevents us from studying the radius instead of the curvature, as will be explained below.

In the case of the spacelike pion form factor the data is taken from the CERN NA7 collaboration [10]. The more recent data from JLAB [11] was taken at values of Q^2 too large for our study. For a recent review on the status of the spacelike form factor see Ref. [12].

The two-loop chiral perturbation theory (χPT) analysis of [13] yielded a mean quadratic radius of

$$\langle r^2\rangle = 0.452(13)\ \mathrm{fm}^2\ , \tag{3}$$

which is the currently accepted value [14]. In order to get a feeling on what to expect for the quartic radius, we start with some simple classical examples. For this discussion we will divide it by the mean square radius squared, the resulting ratio $R \equiv \langle r^4\rangle/\langle r^2\rangle^2$ quantifies the radial spread of the charge distribution. For a charge conducting sphere the spread is minimal with $R = 1$ (all the charge is at the surface), and for a uniformly charged dielectric sphere $R = 25/21$. On the other hand, the ratio is as large as $5/2$ for a charge distribution with an exponential dependence on the radius e^{-mr}. A vector-meson pole form factor

$$F(t) = \frac{1}{1 - t/m_\rho^2}$$

gives an even higher value of $10/3$ [2].

Some results about the pion's quartic radius, including this work, is collected in table 1. Furthermore, after having analyzed the pion em form factor data by using analyticity, the curvature was constrained in the range $[0.25\ \mathrm{GeV}^{-4}, 7.57\ \mathrm{GeV}^{-4}]$ in Ref. [18] and $[2.3\ \mathrm{GeV}^{-4}, 5.4\ \mathrm{GeV}^{-4}]$ in a very recent analysis [19]. Of particular interest for us, and for a lattice determination, is the quark mass dependence, or m_π dependence, of the quartic radius. A study of this within chiral perturbation theory would require control of the N^{3}LO Lagrangian, since the quartic radius is NNLO itself, and this seems out of today's reach.

We examine the problem with the simplifying assumption that $g_{\rho\pi\pi}$ is m_π–independent while the m_π dependence of m_ρ is taken from other sources. To control the model dependence, we employ the Omnès representation of the form factor, sketched in Subsection 2.1 below. In the absence of form factor zeroes, and

neglecting inelastic channels, this only requires knowledge of the elastic pion–pion scattering phase shifts. We parametrize them, with a simple Breit–Wigner model described in Subsection 2.3. Since this model contains $g_{\rho\pi\pi}$ and m_ρ as the only parameters, the above assumption can be employed in a straightforward way. In addition we also use the predictions of unitarized chiral perturbation theory for both rho mass and coupling. The resulting quark mass dependence of the rho properties were investigated in Ref. [5]. Using this alternative parametrization we get almost identical results. The pion mass dependence of the curvature turns out to be similar to that of the square radius.

2. Omnès representation of the form factor

2.1. *Basics*

The Omnès equation [20] encodes the analyticity properties of the pion form factor $F(s)$, that has an elastic unitarity cut on the positive s-axis for $s \in (4m_\pi^2, \infty)$, and is otherwise analytic. Further superimposed cuts due to inelastic channels are neglected in its derivation, and the form factor is assumed to have no zeroes (which, as we know today, is phenomenologically correct). We have explored the possibility of zeroes in the complex plane by analytically continuing the experimental data with the help of the Cauchy–Riemann equations [21]. For a small band around the real axis, they can be excluded. Some remarks on inelastic channels can be found in [22].

The starting point is the well known relation $\mathrm{Im}(F) = \tan\delta_{11}\mathrm{Re}(F)$, which relates the discontinuity in the vector form factor to the elastic scattering phase shift in the vector–isovector channel. From this relation the Watson theorem follows straightforwardly. Since the large-q^2 asymptotic behavior of the form factor is known from QCD counting rules [23], $F(q^2) \to c/q^2$, as a matter of principle one may write an unsubtracted dispersion relation, which reads for arbitrary t

$$F(t) = \frac{1}{\pi} \int\limits_{4m_\pi^2}^{\infty} ds \tan\delta_{11}(s) \frac{\mathrm{Re}(F(s))}{s - t - i\epsilon} \ . \tag{4}$$

We specified "as a matter of principle" since the QCD counting rules apply only when elastic scattering is irrelevant by the numerous inelastic channels open. However, in this work we only want to use low energy input (up to 1.2 GeV) and we will therefore use a subtracted dispersion relation below and cut the high energy contributions with a cut–off. The variation of the results with this cut–off provides a systematic uncertainty in our work, which, as a consequence of the subtraction, turns out to be moderate.

If there are no bound state poles, as is the case of $\pi\pi$ scattering for physical quark masses, nor the form factor vanishes anywhere in the complex plane, as we presume for $F(t)$, the celebrated solution family of this equation provides a representation of the form-factor in terms of the scattering phase, known as the Omnès representation. The standard treatment proceeds by deriving an integral equation for $\log F(t)/(2i)$ instead of $F(t)$ itself,

$$\log\frac{F(t)}{2i} = \frac{1}{2\pi i} \int\limits_{4m_\pi^2}^{\infty} \frac{ds}{s-t} \left(\log\frac{F(s+i\epsilon)}{2i} - \log\frac{F(s-i\epsilon)}{2i} \right) = \frac{1}{\pi} \int\limits_{4m_\pi^2}^{\infty} \frac{ds}{s-t} \delta_{11}(s) \ . \tag{5}$$

Instead of this relation we may use a subtracted version. This will allow us to effectively suppress the high energy behaviour of the phase shifts. In particular we will use a twice subtracted version which reads after exponentiation

$$F(t) = \exp\left(P_1 t + \frac{t^2}{\pi} \int\limits_{4m_\pi^2}^{\infty} ds \frac{\delta_{11}(s)}{s^2(s - t - i\epsilon)} \right) \ . \tag{6}$$

Note, the normalization condition of the form factor prohibits a constant term in the exponent. The constant P_1 can be identified with the square radius of the pion

$$P_1 = \langle r^2 \rangle / 6 \ .$$

This representation of the form factor has been used in the literature, see for example [24].

2.2. *Phase–shift representation of the quartic radius*

Recalling the definition of the curvature of the pion form factor (c.f. Eq. (2)) we may read off an expression for c_V^π directly from Eq. (6):

$$c_V^\pi = \frac{\langle r^4 \rangle}{120} = \frac{1}{72}\langle r^2 \rangle^2 + \frac{1}{\pi} \int\limits_{4m_\pi^2}^{\infty} ds \frac{\delta_{11}(s)}{s^3} \tag{7}$$

which is quite a beautiful formula, since it allows a third independent extraction of the curvature c_V^π besides NNLO χPT or a fit to spacelike data beyond the linear fall in t where uncertainties get large. Instead we employ only the elastic phase shift. In addition, since the quantity

$$\tilde{c}_V^\pi \equiv c_V^\pi - \frac{1}{72}\langle r^2 \rangle^2 \tag{8}$$

is described solely in terms of the $\pi\pi$ p–wave phase shifts, its quark mass dependence is closely linked to that of the ρ–meson properties. This relation is analogous to others existing for the mean–square radius [2,25].

2.3. *A simple Breit–Wigner model*

To provide an estimate of the form factor based on the Omnès representation, we employ a simple relativistic Breit–Wigner model of the scattering amplitude, in which an s–channel resonance dominates the scattering

$$a_{11}(s) = \frac{c}{s - m_\rho^2 - i m_\rho \Gamma_{\rm tot}(s)} \tag{9}$$

where $\Gamma_{\rm tot}$ is the total width of the ρ resonance with

$$\Gamma_{\rm tot} = \frac{g_{\rho\pi\pi}^2 p^3}{6\pi m_\rho^2} = \frac{g_{\rho\pi\pi}^2 (\frac{s}{4} - m_\pi^2)^{3/2}}{6\pi m_\rho^2} \ . \tag{10}$$

We neglected terms of order $\Gamma_{\rm tot}^2$. Here c is an irrelevant constant that may be expressed in terms of m_ρ and $\Gamma_{\rm tot}$. We may write

$$\delta_{11}(s) = \arctan \frac{{\rm Im} a_{11}(s)}{{\rm Re} a_{11}(s)} = \arctan \frac{m_\rho \Gamma_{\rm tot}(s)}{m_\rho^2 - s} \ . \tag{11}$$

With this phase variation the integral representation converges without additional subtractions (although the high–energy tail is ad-hoc), however, even values as large as $s = 7$ GeV^2 contribute to the integral.

A good fit can be seen in Fig. 1 for the phase shift and square form–factor modulus. To produce the figures we use $m_\pi^{\rm phys} = 139$ MeV, $m_\rho = 775$ MeV, $\Gamma_\rho^{\rm phys} = 150$ MeV (to determine $g_{\rho\pi\pi}$).

Using the formula given above we may now extract the curvature directly from the elastic pion phase shifts, using the square radius as input. We find

$$c_V^\pi = 3.75 \pm 0.33 \ {\rm GeV}^{-4} \ , \tag{12}$$

where the uncertainty contains both the uncertainty in $\langle r^2 \rangle$ and the systematic uncertainty introduced by evaluating the integral only up to finite values (we allow a large range from 1 GeV to 16 GeV for the

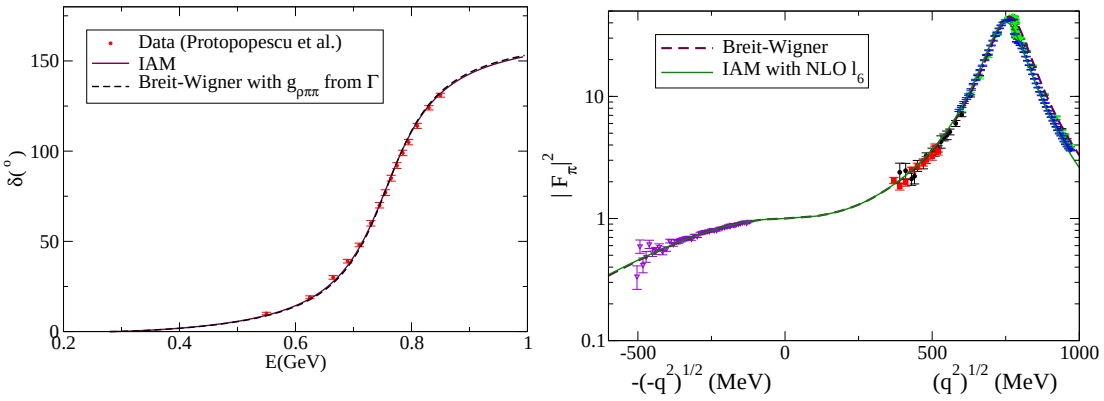

Fig. 1. The scattering phase in the vector channel (left) for the Breit–Wigner model (dashed line) and the Inverse Amplitude Method (solid line). We also plot the square form factor modulus (right). To be able to plot the spacelike and timelike data together, the first is plotted against the unphysical variable $-\sqrt{-q^2}$ with q^2 the (negative) spacelike momentum transfer. Here we use $\langle r^2\rangle$ as input as described in the text.

variation of the cut–off, although the integral is basically converged for a cut–off of 2 GeV). It agrees to that from vector meson dominance which is about 3.5 GeV^{-4} [2] and it is consistent with the constraint [2.3 GeV^{-4}, 5.4 GeV^{-4}] from analyzing the form factor data using analyticity [19]. The advantage of our analysis is that it allows in addition for a controlled estimate of the uncertainty. Equivalently, the result in term of quartic radius is

$$\langle r^4\rangle = 0.68 \pm 0.06 \text{ fm}^4 \ . \tag{13}$$

As mentioned above we will investigate the quark mass dependence of the pion form factor based on the assumption that $g_{\rho\pi\pi}$ is independent of the quark mass with the m_π dependence of m_ρ taken from other sources. Since both parameters are explicit in the parametrization given above, we may study the resulting quark mass dependence of c_V^π, once that of $\langle r^2\rangle$ is fixed.

3. Chiral perturbation theory

3.1. *General considerations*

In order to determine the quark mass dependence of the square radius, which is the input needed for the formalism described above, we will use the results of χPT. Clearly, the curvature c_V^π as well as its quark mass dependence, could also be determined in χPT directly. Depending on the fit and systematics chosen in Ref. [16], which is two–flavor $\mathcal{O}(p^6)$ χPT calculation, its value could vary between $2-6$ GeV^{-4}, although the authors quote a value around 4 GeV^{-4}, in agreement with a previous estimate [2] (By fitting to form factor data, they obtain 3.85 GeV^{-4}). A $\mathcal{O}(p^6)$ fit in three–flavor χPT leads to a range 4.49 ± 0.28 GeV^{-4} [13]. Adopting $c_V^\pi = 4 \pm 2$ GeV^{-4} as the NNLO χPT result, we obtain $\langle r^4\rangle/\langle r^2\rangle^2 = 4 \pm 2$. This value is copied into Table 1.

3.2. *Matching the Omnès representation*

We start by giving the chiral expansion of the vector form factor [26] valid to NLO in χPT,

$$F(t) = 1 + \frac{1}{6f_\pi^2}(t - 4m_\pi^2)\bar{J}(t) + \frac{t}{96\pi^2 f_\pi^2}(\bar{l}_6 - \frac{1}{3}) \ . \tag{14}$$

(To this order we are free to change $M,\ F$ to the physical m_π, f_π, since the difference is of NNLO). In this expression,

$$\bar{J}(t) = \frac{1}{16\pi^2}\left[\sigma \log\left(\frac{\sigma-1}{\sigma+1}\right) + 2\right] \tag{15}$$

with $\sigma = \sqrt{1-4m_\pi^2/t}$. A common strategy is to fix the $\bar{l}_6$ constant from the square charge radius [26]

$$\langle r^2\rangle = \frac{1}{16\pi^2 f_\pi^2}(\bar{l}_6 - 1) \tag{16}$$

which is correct up to $\mathcal{O}(m_\pi^2)$ in χPT. Higher orders in the chiral expansion cannot bring in powers of t since, by definition, the charge squared radius is proportional to the coefficient of the term linear in t in the form factor. However, they can bring additional constants to the right hand side (each of a natural order suppressed by additional factors of $1/(4\pi f_\pi)^2$), and, more important for our purposes, a polynomial of m_π^2. To make sure we are not eschewing a critical m_π dependence, we will compare the right-hand-side of eq.(16) with the NNLO correction in chiral perturbation theory [16]. The NLO result eq. (16), that depends only logarithmically on the pion mass (see eq. (20) below), is then extended to

$$\langle r^2\rangle = \frac{1}{16\pi^2 f_\pi^2}\left[\left(1 + \frac{m_\pi^2}{8\pi^2 f_\pi^2}\bar{l}_4\right)(\tilde{l}_6 - 1) + \frac{m_\pi^2}{16\pi^2 f_\pi^2}\left(16\pi^2\frac{13}{192} - \frac{181}{48}\right)\right] \tag{17}$$

with

$$\tilde{l}_6 = \bar{l}_6 + 6\frac{m_\pi^2}{f_\pi^2}\left[16\pi^2 r_{V1}^r(\mu^2) + \frac{1}{48\pi^2}\log\left(\frac{m_\pi^2}{\mu^2}\right)\left(\frac{19}{12} - \bar{l}_1 + \bar{l}_2\right)\right] \tag{18}$$

where r_{V1}^r is a counterterm to be determined empirically, and we will use the simple VMD estimate from the same work, at the ρ scale,

$$r_{V1}^r(m_\rho^2) \simeq -0.25\times 10^{-3}\ .$$

With this estimate, those authors find

$$\tilde{l}_6 = \bar{l}_6 - 1.44$$

(the scale–dependence of this number cancels in Eq. (18). The estimate is taken with constants corresponding to set I that we copy in Table 2).

Here we have to recall the pion mass dependence of the $\bar{l}$'s. The l_i, as coefficients of the expansion in powers of m_π^2 of the Lagrangian density, are by definition pion–mass independent, and so are their renormalized counterterms l_i^r. However, the barred quantities are related to them by absorbing a chiral logarithm

$$l_i^r = \frac{\gamma_i}{32\pi^2}\left[\bar{l}_i + \log\left(\frac{m_\pi^2}{\mu^2}\right)\right] \tag{19}$$

that makes the $\bar{l}$'s scale–independent, but in exchange, pion–mass dependent. This dependence needs to be kept track of in the calculation. It becomes crucial in the chiral limit when the pion radius diverges due to the virtual pion cloud becoming long–ranged as the pion mass vanishes. This effect appears through $\bar{l}_6$.

Therefore, we denote by $\bar{l}_i^{\rm phys}$ the value that the low energy constants take by fitting to physical–world data. From here on, when varying the quark (or pion) mass, one needs to change the constant according to

$$\bar{l}_i = \bar{l}_i^{\rm phys} - \log\left(\frac{m_\pi^2}{(m_\pi^{\rm phys})^2}\right) \tag{20}$$

With this we have all the input ready to use Eq. (7) also to establish the quark mass dependence of the curvature using the Breit–Wigner representation of the phase shifts and the given assumptions on the quark mass dependence of both the ρ mass and coupling.

However, before we proceed we introduce a method that allows one to estimate the quark mass dependence of the ρ properties directly from the χPT amplitudes evaluated up to a given order, namely the unitarized

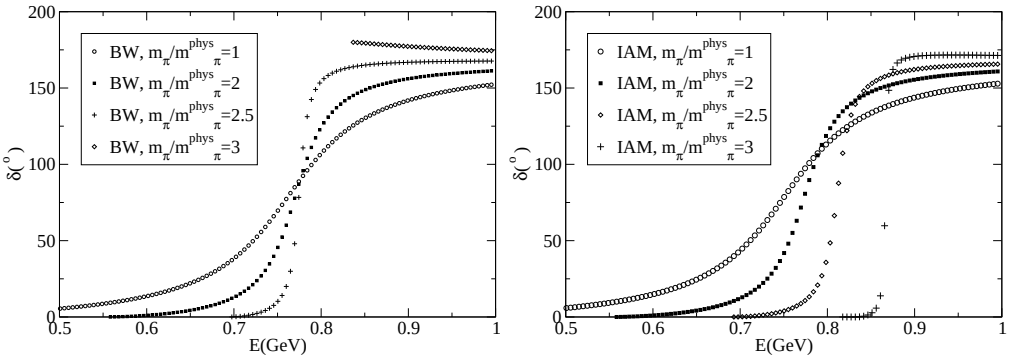

Fig. 2. Variation of the elastic $\pi\pi$ phase δ_{11} with the pion mass. Left: Breit–Wigner model. Note that for $m_\pi = 3m_\pi^{\rm phys}$ the ρ (held at constant mass) has already crossed below the $\pi\pi$ threshold and is a bound state. Right: Inverse Amplitude Method. The resonance stays above the $\pi\pi$ threshold, its mass having a slight dependence on m_π, until rather high pion masses.

chiral perturbation theory or the inverse amplitude method (IAM). The representation we are going to use is consistent with NLO chiral perturbation theory at low momentum, and satisfies exact elastic unitarity, fitting the pion scattering data up to 1.2 GeV well. The formalism will be introduced in the next subsection.

3.3. *P-wave $\pi\pi$ scattering*

To derive the expression for the IAM one starts with the on–shell $\pi\pi$ scattering amplitude in NLO χPT that, for $I = 1$, is

$$A_1(s,t,u) = A(t,s,u) - A(u,t,s) \tag{21}$$

with

$$\begin{aligned} A(s,t,u) = &\frac{s-m_\pi^2}{F^2} + \frac{1}{6F^4}\left[3\bar{J}(s)\left(s^2-m_\pi^4\right) + \bar{J}(t)\left(t(t-u) - 2m_\pi^2 t + 4m_\pi^2 u - 2m_\pi^4\right)\right. \\ &\left. + \bar{J}(u)\left(u(u-t) - 2m_\pi^2 u + 4m_\pi^2 t - 2m_\pi^4\right)\right] + \frac{1}{96\pi^2 f_\pi^4}\left[2\left(\bar{l}_1 - \frac{4}{3}\right)\left(s-2m_\pi^2\right)^2\right. \\ &\left. + \left(\bar{l}_2 - \frac{5}{6}\right)\left(s^2 + (t-u)^2\right) - 3m_\pi^4\bar{l}_3 - 12m_\pi^2 s + 15m_\pi^4\right]. \end{aligned} \tag{22}$$

The first term can be identified as the leading order, low–energy theorem [27], but we express it in terms of the physical m_π, instead of its leading order value M used in the original expression [26]. At the meanwhile, we keep the m_π independent pion decay constant F. The quantities F and M are related to the physical ones via

$$F = f_\pi\left(1 - \frac{m_\pi^2}{16\pi^2 f_\pi^2}\bar{l}_4\right), \quad M^2 = m_\pi^2\left(1 + \frac{m_\pi^2}{32\pi^2 f_\pi^2}\bar{l}_3\right).$$

The latter expression introduces $\bar{l}_3$ into the last line of Eq. (22).

The projection to the spatial p–wave has the usual factor of $1/2$ to avoid double–counting quantum states by counting all angular configurations with exchanged identical particles

$$a_{11}(s) = \frac{1}{32\pi}\frac{1}{2}\int_{-1}^{1} d\cos\theta(\cos\theta) A_1(s, t(s,\cos\theta), u(s,\cos\theta)) \ . \tag{23}$$

One can organize the chiral expansion as

$$a_{11}(s) = a_{11}^{\rm LO}(s) + a_{11}^{\rm NLO}(s) + \ \ldots \tag{24}$$

Table 2
Values of the low energy constants of the NLO SU(2) Chiral Lagrangian. We employ the last row in the calculation. For comparison we give several well–known sets. The error refers to the last significant figure. These are determinations based on data alone. Several phenomenological and theoretical predictions based on semi-analytical approaches (large N_c, Dyson–Schwinger, resonance saturation, etc.) can be found in the literature [31].

LEC	$\bar{l}_1$	$\bar{l}_2$	$\bar{l}_3$	$\bar{l}_4$	$\bar{l}_6$
Gasser-Leutwyler [26]	-2 ± 4	6 ± 1.3	2.9 ± 2.4	4.3 ± 0.9	16 ± 1
Dobado *et al.* [33]	-0.6 ± 0.9	6.3 ± 0.5	2.9 ± 2.4	4.3 ± 0.9	16 ± 1
Bijnens *et al.* set I [16]	-1.7	6.1	2.4	4.4 ± 0.3	16 ± 1
Bijnens *et al.* set II [16]	-1.5	4.5	2.9	4.3	
This work	0.1 ± 1.5	6 ± 1.3	2.9(fix)	4.3 ± 0.9	16.6 ± 0.4

but the series truncated at any order only satisfies elastic unitarity perturbatively. This is solved, with the first two expansion terms, by the Inverse Amplitude Method [28] that reads (suppressing the spin and isospin subindices)

$$a^{\rm IAM}(s) = \frac{a^2_{\rm LO}(s)}{a^{\rm LO}(s) - a^{\rm NLO}(s)} \ . \tag{25}$$

A Taylor expansion of this amplitude returns NLO χPT as usual for a Padé approximant. However elastic unitarity is now exact, and the possibility of a zero of the denominator allows for resonances to appear.

The associated phase shift

$$\delta^{\rm IAM}_{11}(s) = \arctan\left(\frac{{\rm Im}a^{\rm IAM}_{11}(s)}{{\rm Re}a^{\rm IAM}_{11}(s)}\right)$$

may be directly employed for the time–like form factor through the Omnès representation. A similar procedure was taken to calculate the scalar and vector form factors of the pion [29,30].

The pion mass dependence of the ρ meson properties were studied in Ref. [5] and it was found that $g_{\rho\pi\pi}$ depends only very mildly on the quark mass. In the next section we will investigate the consequences of this finding on the pion vector form factor.

The low energy constants necessary to complete the calculation are fit to the phase shifts data and given in Table 2, where they are compared to well–known determinations. Note that with the phase shift data one can only determine the difference $\bar{l}_2 - \bar{l}_1$ which is about 6 as a result of the fitting [32]. Using Eq. (7), the curvature can then be obtained as

$$c_V^\pi = 4.00 \pm 0.50 \ {\rm GeV}^{-4}, \tag{26}$$

or equivalently,

$$\langle r^4 \rangle = 0.73 \pm 0.09 \ {\rm fm}^4. \tag{27}$$

The quantity depending solely on the phase shift is

$$\tilde{c}_V^\pi = 2.13 \pm 0.42 \ {\rm GeV}^{-4}. \tag{28}$$

These values are to be considered as our results at the physical pion mass.

4. Pion-mass dependence needed for lattice extrapolation

4.1. *Mass dependence of the phase shift*

In this section we study the pion mass dependence of the pion vector form factor based on both the Breit–Wigner model as well as the amplitudes from the IAM. In the left panel of Fig. 2 we plot the variation in the isospin–1 p–wave elastic $\pi\pi$ phase shift δ_{11} with the pion mass in the Breit–Wigner model, where

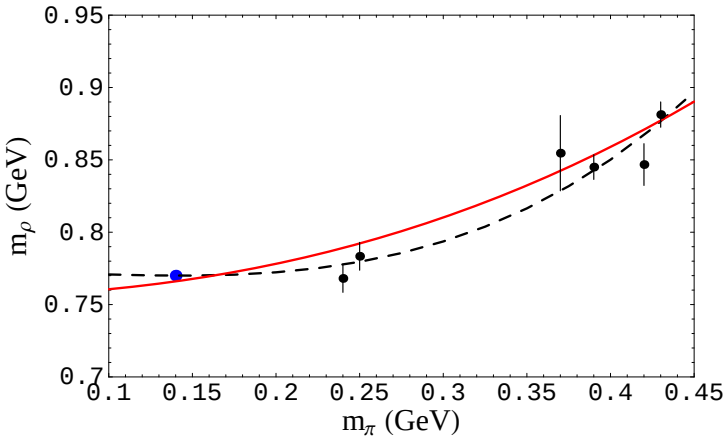

Fig. 3. Dependence of the ρ mass on the pion mass. Here the ρ mass is defined as the value of $\sqrt{s}$, where the $\pi\pi$ p–wave phase shifts cross 90 degrees. Shown are the result from the IAM (solid line) and a fit using Eq. (29) (dashed line) to the lattice data, shown as solid dots [4]. The lowest point is the physical ρ mass.

the physical pion mass is denoted by $m_\pi^{\rm phys}$. For small increases in the pion mass, with m_ρ being held fixed for illustration, we see how the resonance becomes narrower as the pion threshold approaches. Finally, for $2m_\pi > m_\rho$, the ρ becomes bound and the phase shift starts at 180 degrees in agreement with Levinson's theorem with one bound state.

Next we consider the IAM. Here what is held constant is the renormalized constants in the chiral Lagrangian ($l_i^r(\mu)$) since, as discussed, they are by definition independent of the pion mass. The scale–independent $\bar{l}'s$ run logarithmically with the pion mass. This dependence and the explicit pion masses in the chiral series bring about a small m_π–dependence of the ρ mass that puts it just above threshold for $m_\pi = 3m_\pi^{\rm phys}$. We plot in the right panel of Fig. 2 the resulting phase as a function of the $\pi\pi$ invariant mass for different values of the pion mass.

The prediction of the pion mass dependence of the ρ mass resulting from the IAM is shown as the solid curve in Fig. 3. The parameters used are $\bar{l}_1 = -0.08, \bar{l}_2 = 5.78, \bar{l}_3 = 2.9$ and $\bar{l}_4 = 4.3$. In this figure we also show the results of a recent lattice study [4]. For our comparison we choose this one, for it is the simulation where the lowest pion masses are used. To allow for a comparison with recent lattice data, here the ρ–mass is defined as the value of $\sqrt{s}$, where the $\pi\pi$ phase shift is 90°. The resulting numbers differ somewhat from those corresponding to the real part of the pole position in the second Riemann sheet — the latter definition of the mass was used in Ref. [5]. For comparison, we also show the very recent lattice data [4] as the filled circles with error bars. The agreement of the IAM with the lattice data is rather satisfying. For later use, the lattice data are fitted with an expression derived from an extended version of χPT [36]

$$m_\rho = m_\rho^0 + c_1 m_\pi^2 + c_2 m_\pi^3 + c_3 m_\pi^4 \log\left(\frac{m_\pi^2}{m_\rho^2}\right) \ . \tag{29}$$

The parameter m_ρ^0 is not included in the fit. It is fixed by the condition that $m_\rho = 0.77$ GeV at the physical pion mass. We find for the ρ mass in the chiral limit $m_\rho^0 = 0.77 \pm 0.1$ GeV. The resulting parameters are

$$c_1 = -0.53 \pm 0.44 \ {\rm GeV}^{-1}, \quad c_2 = 2 \pm 1 \ {\rm GeV}^{-2}, \quad c_3 = -1 \pm 3 \ {\rm GeV}^{-3}. \tag{30}$$

Using the central values, we get the dashed curve as shown in Fig. 3. Note, the uncertainties in the parameters show some correlation, however, since we are here mainly interested in a parametrization of the lattice data, we may ignore this observation. Since the pion mass grows faster with the quark mass, eventually the ρ becomes bound (just as the J/ψ is under the $D\bar{D}$ threshold), but this happens for yet larger pion masses.

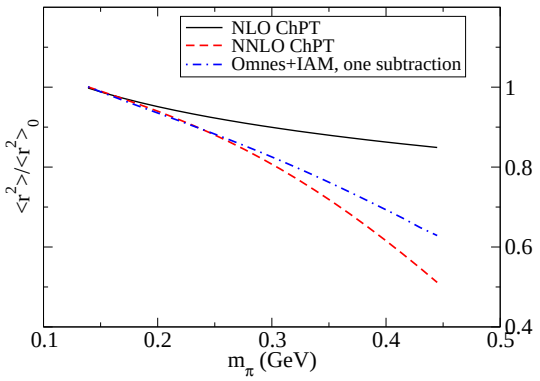

Fig. 4. Pion mass dependence of the mean square radius. We show results based on NLO and NNLO Chiral Perturbation theory. The r^r_{V1} parameter is fixed at its VMD value (its pion-mass dependence contributing at NNNLO is neglected). Likewise we plot the mass dependence resulting from a once-subtracted Omnès representation. The data is normalized to the radius for physical pion mass.

4.2. *Extrapolation in NLO and NNLO chiral perturbation theory*

Space–like form factors are in principle accessible on a lattice. Since these studies usually employ heavier-than-real quarks, the pion mass obtained is also higher than the physical pion mass, and an extrapolation is necessary. Another extrapolation to low momentum (due to the finite volume enclosed by the lattice) is necessary if the mean square and quartic radii are to be extracted. The mean square radius has indeed been studied before [15,34] and extrapolation to physical pion masses taken from chiral perturbation theory. It would be interesting to have lattice data at several quark masses to test it.

Momentum extrapolations to $q^2 = 0$ are, in view of the mean quartic radius, non-linear. In the extraction of the mean square radius, the authors of [34] quote a 10% systematic error in the lattice extraction due to $m_\pi^2/(1\ \mathrm{GeV}^2)$ χPT errors, and 20% due to $q^2_{\mathrm{min}}/(1\ \mathrm{GeV}^2)$ momentum extrapolation errors.

The momentum extrapolation however seems to be avoidable with twisted boundary conditions for the fermion fields [15], and indeed those authors find

$$\langle r^2\rangle_{330\ \mathrm{MeV}} = 0.35(3)\ \mathrm{fm}^2, \quad \langle r^2\rangle_{139\ \mathrm{MeV}} = 0.42(3)\ \mathrm{fm}^2\ .$$

where the value at the physical pion mass is obtained with the help of the NLO $SU(2)$ chiral Lagrangian.

4.3. *Chiral extrapolation assisted by the Omnès representation*

We have achieved a representation of the form factor based on the Omnès representation, matched to low energy χPT. Since we have relatively good theoretical control of the entire construction, we can now extrapolate to unphysical quark (pion) masses.

The parametrization in Eq. (7) requires two pieces of input: the pion scattering p–wave phase shift and the mean square radius. For the former we may either use the Breit–Wigner model – together with additional assumptions on the ρ properties – or the IAM, where the quark mass dependence is predicted from NLO χPT – higher order pion mass dependencies as they arise from NNLO χPT are not yet studied in this framework.

The square radius has a NLO pion mass dependence caused by the chiral logarithm in $\bar{l}_6$. This is a major effect for pion masses smaller than physical, towards the chiral limit, but for pion masses higher than physical (say the 330 MeV where the lattice data is taken), the m_π^2 term from the NNLO Lagrangian density might come to dominate, so we employ this too. Finally, we have an order-of-magnitude countercheck at our disposal. By employing a once–subtracted instead of a twice–subtracted Omnès representation, we obtain a closed form for the mean square radius in terms of the phase shift

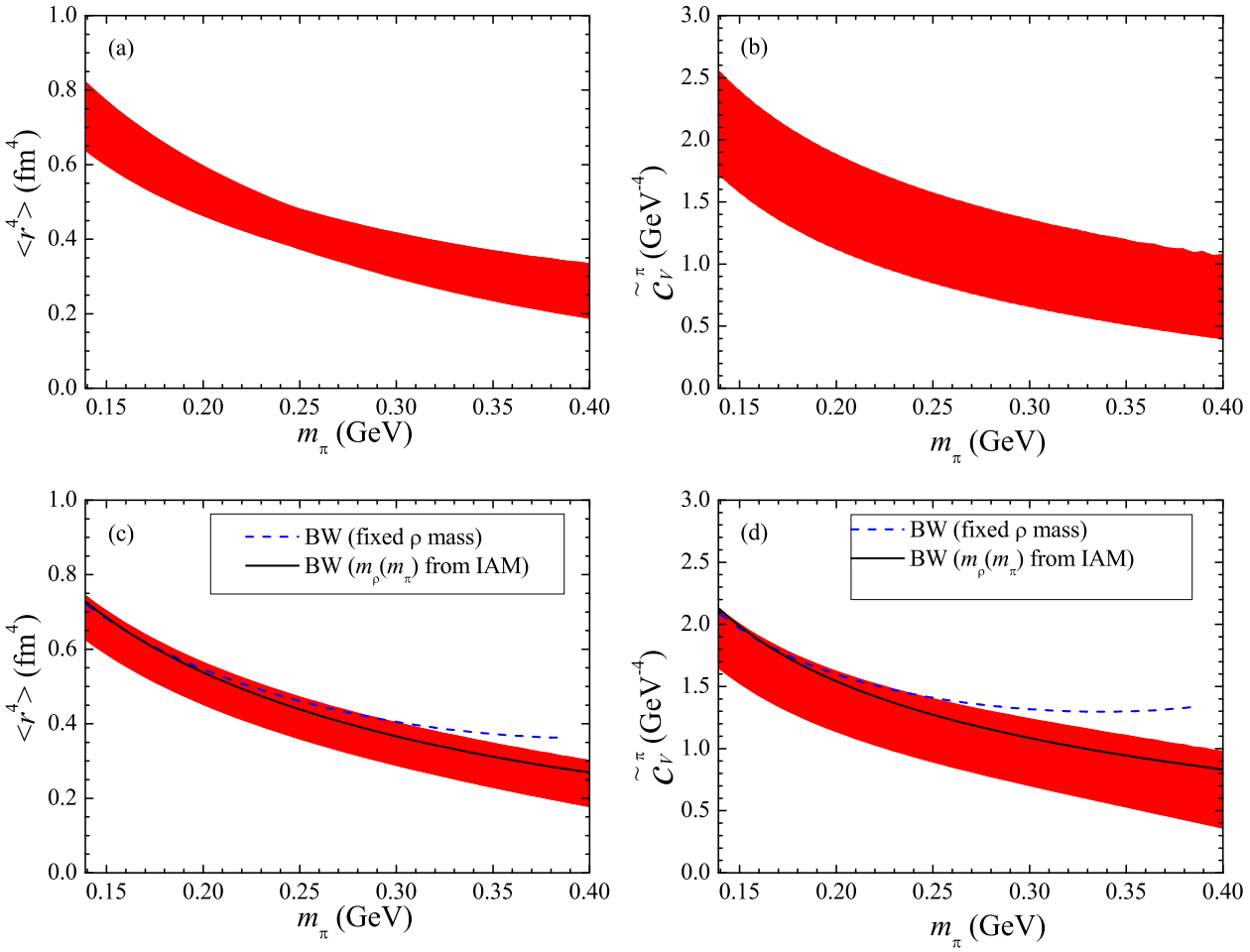

Fig. 5. Dependence on the pion mass of the mean quartic radius of the pion (left panel) and $\tilde{C}_V^\pi$ (right panel). We show results based on the Breit–Wigner model and the Inverse Amplitude Method. The bands correspond to the uncertainties from the parameters used (the $\bar{l}_i$'s for the IAM and the c_i (c.f. Eq. (29)) for the Breit-Wigner) as well as from the variation of the cut–off.

$$\langle r^2 \rangle = \frac{6}{\pi} \int_{4m_\pi^2}^{\infty} ds \frac{\delta_{11}(s)}{s^2} \ . \tag{31}$$

All three methods are plotted in Fig. 4.

The results of the pion mass dependence of the quartic radius using the Breit–Wigner model and the IAM are plotted in Fig. 5(a) and (c), respectivley, with the m_π dependence of the square radius coming from that of $\bar{l}_6$ as dictated by Eq. (20). In the IAM, the pion mass dependence of m_ρ is included intrinsically, while in the Breit–Wigner method, it is input from fitting to the recent lattice data [4] as described at the end of Subsection 4.1. The bands include the uncertainty from varying the parameters within one sigma and that from varying the integration cut–off from 1 to 16 GeV. The uncertainty from the cut–off is the dominant one. For comparison, we also plot the result of the Breit–Wigner model with fixed ρ mass as the dashed curve in Fig. 5(c). The dependence is smooth up to the point when the rho becomes stable. Here the curve ends. Imposing the m_π–dependent ρ mass as that given by the IAM, the result for the quartic radius in the Breit–Wigner model is shown as the solid curve in Fig. 5(c).

We can dispose altogether from the explicit pion mass dependence in $\langle r^2 \rangle$ by studying the quantity

$$\tilde{c}_V^\pi = c_V^\pi - \frac{1}{72}\langle r^2\rangle^2.$$

This constant $\tilde{c}_V^\pi$ can of course be also studied on a lattice by itself, although its physical interpretation is not transparent. But its mass dependence comes from the phase shift alone (c.f. Eq. (8)), and is not compounded with the mass dependence of the square radius. It is therefore this quantity that allows most directly access to the pion mass dependence of the ρ properties. Our results for this quantity are shown in Fig. 5(b) and (d) using the IAM and the Breit–Wigner model, respectively.

5. Summary

Using the Omnès representation for the pion vector form factor, in this paper we improved the existing value for the corresponding curvature using as input only the well known $\pi\pi$ phase shifts in the p–wave as well as the pion radius. We find $\langle r^4\rangle = 0.73 \pm 0.09$ fm^4 or equivalently $c_V = 4.00 \pm 0.50$ GeV^{-4} which are consistent with the results from NNLO χPT [16,13] and recent analysis using analyticity [19].

In addition we studied the pion mass dependence of the curvature. A modification of the curvature, called $\tilde{c}_V^\pi$ in the paper, can be represented solely by the $\pi\pi$ p–wave phase shift. We argued that this quantity allows for a clean and model–independent alternative access to the pion mass dependence of the ρ properties and would therefore provide a consistency check of the methods to extract physical parameters from lattice simulations. A lattice QCD study of the pion curvature would therefore be of high theoretical interest. We also argued that the pion square radius is not well suited for this kind of investigation, since additional, not so well controlled, theoretical input would be needed in the analysis. Quantities similar to $\tilde{c}_V^\pi$ exist also for other form factors, and a study of them from both theoretical and lattice sides would be interesting.

We would like to thank Stephan Dürr and Jose Pelaez for useful discussions. This work is supported in part by grants FPA 2004-02602, 2005-02327, FPA2007-29115-E (Spain), and by the Helmholtz Association through funds provided to the virtual institute "Spin and strong QCD" (VH-VI-231). FJLE thanks the members of the IKP (Theorie) at Forschungszentrum Jülich for their hospitality during the preparation of this work and the Fundacion Flores Valles for economical support.

References

[1] M. E. Rose, Phys. Rev. **73** (1948) 279.
[2] J. Gasser and U.-G. Meißner, Nucl. Phys. B **357** (1991) 90.
[3] S. Aoki *et al.* [CP-PACS Collaboration], Phys. Rev. D **60** (1999) 114508 [arXiv:hep-lat/9902018]; S. Dürr *et al.*, Science **322** (2008) 1224; C. Gattringer, C. Hagen, C. B. Lang, M. Limmer, D. Mohler and A. Schafer, arXiv:0812.1681 [hep-lat]; P. Dimopoulos, C. McNeile, C. Michael, S. Simula and C. Urbach [ETM Collaboration], arXiv:0810.1220 [hep-lat].
[4] M. Gockeler, R. Horsley, Y. Nakamura, D. Pleiter, P. E. L. Rakow, G. Schierholz and J. Zanotti, arXiv:0810.5337 [hep-lat].
[5] C. Hanhart, J. R. Pelaez and G. Rios, Phys. Rev. Lett. **100** (2008) 152001 [arXiv:0801.2871 [hep-ph]].
[6] R. R. Akhmetshin *et al.*, JETP Lett. **84** (2006) 413 [Pisma Zh. Eksp. Teor. Fiz. **84** (2006) 491] [arXiv:hep-ex/0610016]; R. R. Akhmetshin *et al.* [CMD-2 Collaboration], Phys. Lett. B **648** (2007) 28 [arXiv:hep-ex/0610021];
[7] A. Aloisio *et al.* [KLOE Collaboration], Phys. Lett. B **606** (2005) 12 [arXiv:hep-ex/0407048].
[8] M. N. Achasov *et al.*, J. Exp. Theor. Phys. **101** (2005) 1053 [Zh. Eksp. Teor. Fiz. **101** (2005) 1201] [arXiv:hep-ex/0506076].
[9] E. P. Solodov [BABAR collaboration], in *Proc. of the e^+e^- Physics at Intermediate Energies Conference* ed. Diego Bettoni, *In the Proceedings of e+ e- Physics at Intermediate Energies, SLAC, Stanford, California, 30 Apr - 2 May 2001, pp T03* [arXiv:hep-ex/0107027].
[10] S. R. Amendolia *et al.* [NA7 Collaboration], Nucl. Phys. B **277** (1986) 168.
[11] J. Volmer *et al.* [The Jefferson Lab F(pi) Collaboration], Phys. Rev. Lett. **86** (2001) 1713 [arXiv:nucl-ex/0010009].
[12] G. M. Huber, J. Phys. Conf. Ser. **69** (2007) 012015.
[13] J. Bijnens and P. Talavera, JHEP **0203** (2002) 046 [arXiv:hep-ph/0203049].
[14] W. M. Yao *et al.* [Particle Data Group], J. Phys. G **33** (2006) 1.
[15] P. A. Boyle *et al.*, JHEP **0807**, 112 (2008) [arXiv:0804.3971 [hep-lat]].
[16] J. Bijnens, G. Colangelo and P. Talavera, JHEP **9805** (1998) 014 [arXiv:hep-ph/9805389].
[17] P. Masjuan, S. Peris and J. J. Sanz-Cillero, Phys. Rev. D **78** (2008) 074028 arXiv:0807.4893 [hep-ph].

[18] I. Caprini, Eur. Phys. J. C **13** (2000) 471 [arXiv:hep-ph/9907227].
[19] B. Ananthanarayan and S. Ramanan, arXiv:0811.0482 [hep-ph].
[20] R. Omnes, Nuovo Cim. **8** (1958) 316.
[21] M. Gimeno-Segovia and F. J. Llanes-Estrada, Eur. Phys. J. C **56** (2008) 557 [arXiv:0805.4145 [hep-th]].
[22] H. Leutwyler, arXiv:hep-ph/0212324.
[23] S. J. Brodsky and G. R. Farrar, Phys. Rev. D **11** (1975) 1309.
[24] F. Guerrero, Phys. Rev. D **57** (1998) 4136 [arXiv:hep-ph/9801305]; F. Guerrero and A. Pich, Phys. Lett. B **412** (1997) 382 [arXiv:hep-ph/9707347].
[25] J. A. Oller and L. Roca, Phys. Lett. B **651** (2007) 139 [arXiv:0704.0039 [hep-ph]].
[26] J. Gasser and H. Leutwyler, Annals Phys. **158** (1984) 142.
[27] S. Weinberg, Physica A **96** (1979) 327.
[28] A. Dobado, M. J. Herrero and T. N. Truong, Phys. Lett. B **235** (1990) 134.
[29] T. N. Truong, Phys. Rev. Lett. **61** (1988) 2526.
[30] F. Guerrero and J. A. Oller, Nucl. Phys. B **537** (1999) 459 [Erratum-ibid. B **602** (2001) 641] [arXiv:hep-ph/9805334].
[31] G. Ecker, J. Gasser, A. Pich and E. de Rafael, Nucl. Phys. B **321** (1989) 311; F. J. Llanes-Estrada and P. De A. Bicudo, Phys. Rev. D **68** (2003) 094014 [arXiv:hep-ph/0306146]; T. N. Pham and T. N. Truong, Phys. Rev. D **31** (1985) 3027; F. J. Yndurain, arXiv:hep-ph/0212282; M. R. Pennington and J. Portoles, Phys. Lett. B **344** (1995) 399 [arXiv:hep-ph/9409426].
[32] A. Dobado and J. R. Pelaez, Phys. Rev. D **56** (1997) 3057 [arXiv:hep-ph/9604416].
[33] A.Dobado *et al.*, Effective Lagrangians for the Standard Model, Springer-Verlag, Berlin Heidelberg 1997.
[34] T. B. Bunton, F. J. Jiang and B. C. Tiburzi, Phys. Rev. D **74** (2006) 034514 [Erratum-ibid. D **74** (2006) 099902] [arXiv:hep-lat/0607001].
[35] J. F. Donoghue, arXiv:hep-ph/9607351.
[36] P. C. Bruns and U.-G. Meißner, Eur. Phys. J. C **40** (2005) 97 [arXiv:hep-ph/0411223].